Nanosecond Dynamics of Horse Heart Apocytochrome *c* in Aqueous Solution As Studied by Time-Resolved Fluorescence of the Single Tryptophan Residue (Trp-59)†

Michel Vincent,‡ Jean-Claude Brochon,‡ Fabienne Merola,‡ Wilco Jordi,§ and Jacques Gallay*,‡

Laboratoire pour l'Utilisation du Rayonnement Electromagnêtique, Centre National de la Recherche Scientifique, Ministère de l'Education Nationale, Commissariat à l'Energie Atomique, Universitê Paris Sud, Bâtiment 209D, 91405 Orsay, France, and Department of Biochemistry, Rijksuniversiteit Utrecht, Padualaan 8, 3584CH Utrecht, The Netherlands

Received November 20, 1987; Revised Manuscript Received July 15, 1988

ABSTRACT: The time-resolved fluorescence emission characteristics of the single tryptophan residue (Trp-59) of horse heart apocytochrome *c*—the precursor of the intramitochondrial cytochrome *c*—were studied in aqueous solution. The total fl orescence intensity decay measured over the whole emission spectrum was analyzed as a sum of three or four exponentials by the nonlinear least-squares method, the last model always providing a slight but significant decrease in the χ^2 values. Maximum entropy analysis, recently developed for time-resolved fluorometry (Livesey et al., 1987; Livesey & Brochon, 1987), strongly suggests the existence of a distribution including at least four separate classes of lifetimes. The center values were around 0.1–0.2, 1, 3, and 5 ns, in agreement with the lifetime values obtained by nonlinear least-squares regression analysis. As a function of the emission wavelength, these values remained constant within the experimental error, whereas a redistribution of the fractional amplitudes was observed: the contributions of the short components increased in the blue edge region of the emission spectrum. Temperature increase led essentially to a redistribution of the fractional amplitudes, affecting mostly that of the 5-ns component, which almost totally disappeared at high temperature (35–40 °C). The lifetime values were not significantly affected except for the 3-ns component, which decreased by about 15% in the temperature range studied. Such observations strongly suggest that the protein exists under different conformational substates in thermal equilibrium. Time-resolved fluorescence anisotropy measurements evidenced the existence of fast internal rotation of the Trp residue. An average maximum restricted angle of rotation of around 55° was calculated. A second internal motion, slower by 1 order of magnitude, corresponding likely to a local motion of the peptide chain involving the Trp-59 residue, was detected on the anisotropy decay curve. Finally, the longest correlation time (5 ns) should correspond to the average rotation of the overall protein. Its value doubled as a function of the protein concentration, revealing an association process leading most likely to a dimer in the concentration range studied (2–139 μM). The flexibility of the peptide chain was more restrained in the associated than in the monomeric form, but the fast internal rotation of the Trp residue was not.

The single tryptophan residue (Trp-59) and one of the four tyrosine residues (Tyr-48) of horse heart cytochrome *c* play an important role in the interactions of the peptide chain with the heme moiety, as they have been shown to be hydrogen-bonded respectively to each of the two heme propionic acid side chains (Dickerson et al., 1975; Wand & Englander, 1985). This situation in the holoprotein explains its extremely strong quenching (Fisher et al., 1973; Weber & Teale, 1959). X-ray diffraction studies as well as recent NMR data have evidenced the high degree of structural organization of the holoprotein (Dickerson et al., 1975; Wand & Englander, 1985). The removal of the heme group evokes two main effects. First, the secondary structure is lost, as shown by circular dichroism as well as ^{1}H NMR[1] measurements (Fisher et al., 1973; Stellwagen et al., 1972; Cohen et al., 1974). Second, the intrinsic protein fluorescence is strongly enhanced (Fisher et al., 1973; Rietveld et al., 1985). In the apoprotein, the "priviledged" situation of Trp-59 and its strong fluorescence make it a very attractive intrinsic probe for studying the protein flexibility in different environments at a specific and essential location. Such a flexibility is expected to be of great importance for the accommodation of the apoprotein to changing environments during the translocation from the cytoplasmic compartment where it is synthesized to the mitochondrion where the heme group is enzymatically bound (Hennig et al., 1983). In this respect, structural changes have been recently observed by steady-state fluorescence measurements upon interaction of apocytochrome *c* with membrane models (Rietveld et al., 1985; Berkhout et al., 1987). As it is also the case for bioactive peptides, it is of fundamental importance to investigate the possible existence of conformational substates for these unstructured proteins in aqueous solutions (Blundell & Wood, 1982; Schiller, 1985) since they display in their amino acid sequence the potential to fold under specific conditions at a membrane interface (Bornet & Edelhoch, 1971; Schneider & Edelhoch, 1972; Braun et al., 1983; Gremlich et al., 1983; Gallay et al., 1987).

In this work, the time-resolved fluorescence emission of the horse heart apocytochrome *c* Trp-59 was studied in aqueous solution by the time-correlated single photon counting technique using the synchrotron radiation pulses as excitation light source. The total intensity decay data were analyzed by nonlinear least-squares regression and by the maximum en-

† This work was partially supported by Grant CRE 879015 from the Institut National de la Santê et de la Recherche Mêdicale.

* Address correspondence to this author at LURE, UPS, Bat 209D, 91405 Orsay Cedex, France.

‡ Universitê Paris SUD.

§ Rijksuniversiteit Utrecht.

[1] Abbreviations: MEM, maximum entropy method; Apo *c*, horse heart apocytochrome *c*; NMR, nuclear magnetic resonance.

0006-2960/88/0427-8752$01.50/0 © 1988 American Chemical Society

tropy method developed recently for fluorescence spectroscopy (Brochon & Livesey, 1988; Livesey et al., 1987; Livesey & Brochon, 1987). The analysis of the total fluorescence intensity decays suggests the existence of discrete interconvertible environments for the Trp-59. Time-resolved fluorescence anisotropy decay measurements indicate a high degree of rotational freedom for the Trp residue in the protein matrix and a local flexibility of the peptide segment bearing the Trp-59 residue. The fluorescence anisotropy data also reveal a self-association process, reversible by urea addition, leading to likely a dimer in the experimental conditions of pH and ionic strength.

Materials and Methods

Chemicals. The *p*-terphenyl came from Koch-Light (Colnbrook Bucks, England). Cyclohexane, Uvasol grade, and glycerol, spectroscopic grade, were from Merck (Darmstadt, FRG) and Eastman Kodak (Rochester, NY), respectively. Other chemicals were of the highest grade commercially available.

Protein Preparation. Horse heart cytochrome *c* (type VI) was purchased from Sigma (St. Louis, MO). Apocytochrome *c* was prepared as previously described (Fisher et al., 1973; Rietveld et al., 1983). For all measurements, the lyophilized product was dissolved in 0.1 M acetate buffer, pH 5. Protein concentration was determined by using an extinction coefficient of 0.92 mL mg^{-1} at 280 nm (Stellwagen et al., 1972).

Fluorescence Measurements. Corrected fluorescence spectra were obtained on a SLM 8000 spectrofluorometer using a "magic angle" configuration. Excitation was set at 295 nm. Bandwidths of 2 and 4 nm were set at the excitation and emission sides, respectively.

Steady-state anisotropy measurements were performed on the same spectrofluorometer in the T-format configuration as described previously (Vincent et al., 1982). For the measurements of the intrinsic fluorescence anisotropy in vitrified medium as a function of the excitation wavelength, a 1-nm bandwith was used for the excitation and the fluorescence was collected through a 1 M $CuSO_4$ filter (1-cm optical path). A concentration of 10 μM protein in 91% glycerol (v/v) was used throughout. The fluorescence background of glycerol was subtracted.

Time-resolved total fluorescence intensity, $T(t)$, and anisotropy decays, $r(t)$, were measured on the instrument setup of LURE (Jameson & Alpert, 1979; Brochon, 1980) by the time-correlated single photon counting method (Yguerabide, 1972; Wahl, 1975). The excitation pulse on this instrument is provided by the electron storage ring ACO (Anneau de Collision d'Orsay) working at a frequency of 13.6 MHz in a single bunch mode and with a usual measured full width at half-maximum of 1.4 ns. For total intensity decay measurements, $T(t)$, the data accumulation was typically stopped when $\sim 6 \times 10^4$ to 5×10^5 counts were collected in the peak channel. For the monitoring of the transient anisotropy, data collection was stopped when $\sim 10^5$ counts were reached in the peak channel of the difference curve $D(t) = I_{vv}(t) - I_{vh}(t)$. Blank subtraction was performed when needed. The apparatus response function, $E(t)$, was obtained with the lifetime standard *p*-terphenyl in cyclohexane (τ = 0.95 ns at 20 °C; Berlman, 1971) according to the method of Wahl (1979). The $E(t)$ acquisition was stopped when $\sim 10^5$ and $\sim 3 \times 10^5$ counts were collected in the peak channel for $T(t)$ and $r(t)$ experiments, respectively.

Data Analysis. Analysis of $T(t)$ as a sum of exponentials was performed either by a nonlinear least-squares procedure (up to four exponentials) (Grinvald & Steinberg, 1974; Wahl, 1979) or by the maximum entropy method for which the lifetime components are equally spaced in a logarithmic scale (Brochon & Livesey, 1988; Livesey et al., 1987; Livesey & Brochon, 1987). In this work, 150 lifetime values ranging from 0.050 to 20.0 ns were typically used. The principles of MEM as applied to time-resolved fluorescence are outlined in the following. With a vertically polarized light, the parallel $I_{vv}(t)$ and perpendicular $I_{vh}(t)$ components of the fluorescence intensity at time t after the start of the excitation are

$$I_{vv}(t) = \frac{1}{3}E_\lambda(t)^* \int_0^\infty \int_0^\infty \int_{-0.2}^{+0.4} \gamma(\tau,\theta,A)e^{-t/\tau}(1 + 2Ae^{-t/\theta})\, d\tau\, d\theta\, dA \quad (1)$$

and

$$I_{vh}(t) = \frac{1}{3}E_\lambda(t)^* \int_0^\infty \int_0^\infty \int_{-0.2}^{+0.4} \gamma(\tau,\theta,A)e^{-t/\tau}(1 - Ae^{-t/\theta})\, d\tau\, d\theta\, dA \quad (2)$$

where $E_\lambda(t)$ is the temporal shape of the excitation flash and an asterisk denotes a convolution product. $\gamma(\tau,\theta,A)$ represents the number of fluorophores with fluorescence lifetime τ, rotational correlation time θ, and initial anisotropy A. If we are only interested in the determination of the total intensity decay parameters, we can considerably simplify the analysis by summing the parallel and perpendicular components

$$T(t) = I_{vv}(t) + 2I_{vh}(t) = E_\lambda(t)^* \int_0^\infty \alpha(\tau)e^{-t/\tau}\, d\tau \quad (3)$$

where $\alpha(\tau)$ is the distribution of excited-state lifetimes given by

$$\alpha(\tau) = \int_0^\infty \int_{-0.2}^{0.4} \gamma(\tau,\theta,A)\, d\theta\, dA \quad (4)$$

However, the experimental data $I_{vv}(t)$ and $I_{vh}(t)$ are noisy and finite in extent. The analysis will strictly provide an infinite set of $\alpha(\tau)$ solutions within the experimental error. We then choose the distribution that maximizes the Skilling–Jaynes entropy (Jaynes, 1983; Livesey & Skilling, 1985)

$$S = \int_0^\infty \alpha(\tau) - m(\tau) - \alpha(\tau) \log \frac{\alpha(\tau)}{m(\tau)}\, d\tau \quad (5)$$

where $m(\tau)$ is a starting model that is flat in log τ space if the experimentator has no a priori knowledge about the τ values expected (Livesey & Brochon, 1987). In order to ensure our recovered distribution agrees with our data, we maximize S subjected to the constraint

$$\sum_{k=1}^{M} \frac{(T_k^{calc} - T_k^{obs})^2}{\sigma_k^2} \leqslant M \quad (6)$$

where T_k^{calc} and T_k^{obs} are the kth calculated and observed intensities. σ_k^2 is the variance of the kth point ($\sigma_k^2 = \sigma_k^{vv2} + 4\sigma_k^{vh2}$; Wahl, 1979). M is the total number of observations.

The center τ_j of a single class j of lifetimes over the $\alpha_i(\tau_i)$ distribution is defined as

$$\tau_j = \sum_i \alpha_i(\tau_i)\tau_i / \sum_i \alpha_i(\tau_i) \quad (7)$$

the summation being performed on the significant values of the $\alpha_i(\tau_i)$.

Analysis of $r(t)$ was performed by nonlinear least-squares regression (Wahl, 1979).

Simulated Data. Synthetic fluorescence decay curves were generated with regard to the conditions of the experimental data collection, i.e., essentially the same time scale, time resolution, and boundaries. The different data sets were ob-

tained by convoluting an experimental decay of the lifetime standard *p*-terphenyl with a sum of discrete exponentials (3 and 4) or with continuous distributions involving 150 exponentials: Gaussian, double Gaussian, Lorentzian, third-degree polynomial function. The simulated data were scaled from 6×10^4 to 5×10^5 counts in the peak channel and Gaussian noise added to approximate Poisson counting statistics.

RESULTS

Simulated Decay Analysis. In order to investigate the ability of MEM to recover simulated data, we have first constructed the following continuous distributions: Gaussian, Lorentzian, and a third-degree polynomial function that is an envelope of the four narrow species mainly responsible for the fluorescence emission characteristics of the apocytochrome *c* presented in this work. It can be seen in Figure 1 that the 150 amplitude values recovered by MEM are close to the injected ones in the simulations when the iterative process of analysis is stopped at the χ^2 value of the simulation. Moreover, this is correct whatever the counting statistics in the tested range, i.e., from 60 000 counts (data not shown) in the peak channel to 500 000. The slight discrepancy between simulated and recovered profiles observed in the short-lifetime region (Figure 1) can be reasonably ascribed to the fact that for exponential decays of fluorescence, and for a given time resolution, there is more significant channels in the long time region of the decay as compared to the short time one.

When discrete exponentials are used as input data in the simulations, the recovery of these discrete species by MEM is readily achieved up to three components, whatever the counting level (data not shown). When four components are present, it is obvious that the profile obtained by MEM at the χ^2 value corresponding to the simulation depends on the number of counts in the peak channel of the total fluorescence intensity (parts A and D of Figure 2). A less structured profile is obtained for the simulated decay with a maximum of 60 000 counts than for the similar simulation with 500 000 counts in the peak channel. Obviously, the noise to signal ratio has to be strongly minimized when, for instance, four discrete components are expected to be extracted from among 150 assumed ones.

The aim of MEM is to maximize the absolute value of the entropy (in other words, to increase the degree of structuration of the amplitude profile when starting from a flat map model). In the case of the simulated data, there is no problem to stop the analysis at the χ^2 value since this value is known. Theoretically, the same procedure can be applied for raw experimental data, but it is well-known that several distortion factors such as nonstatistical noise, electronic drift of the impulse response, or instrumental nonlinearity are occurring, leading to χ^2 values ranging strictly above 1.0 for significantly cumulated data. Then, the MEM process cannot be stopped on the basis of an expected χ^2 value of 1.0. This is especially crucial for the recovery of the physical distribution since, for instance, when MEM is performed in the simulations below the χ^2 boundary of 1.0, the continuous distributions of Figure 1 can even be structured (data not shown).

To date, in the absence of a satisfying statistical stopping criterion (Skilling, personal communication) able to prevent such an overfitting of experimental fluorescence data, we have used an empirical means essentially based on the amplitude profile stability as a function of the iteration number. This was performed by evaluating the number of significant lifetime components among the 150 ones in the intermediate iterations after free processing of MEM. We assumed first that the contribution of a given time component amplitude was significant when its value was higher than 3% of the maximum of the amplitude profile. After, since we were working during the analysis within a lifetime range from 50 ps to 20 ns, overlapping the values of the simulations and the experimental data, we had also to check the stability of the amplitude profile sides. This was performed every two iterations. When the current number of significant time components remained stable, the number of noncontributing lifetimes on both sides of the amplitude profile did not vary significantly as compared

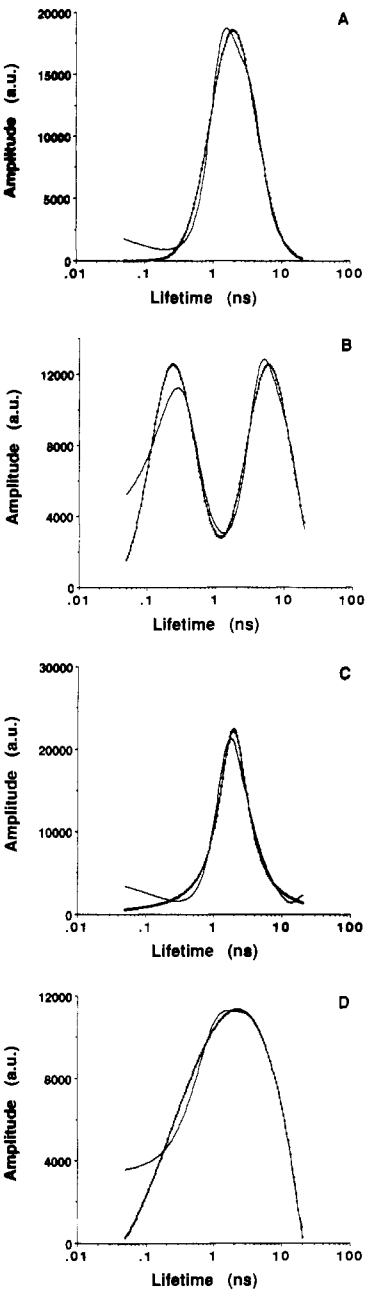

FIGURE 1: Amplitude profiles of the simulated continuous distributions of 150 exponentials recovered by MEM when the analysis is stopped at the χ^2 value of the simulation. 500,000 counts in the peak channel for all simulations. (■) Original simulation. (—) Profile recovered by MEM at the χ^2 value of the simulation. (A) Gaussian logarithmic symmetrical distribution centered at 1.9 ns. Full width at half-maximal was ~5.5 ns. The χ^2 value for this simulation was 1.009. (B) Double-Gaussian logarithmic symmetrical distribution centered at ~0.25 and 6.0 ns. Full width at half-maximum was ~0.6 and 14.0 ns, respectively. The χ^2 value for this simulation was 1.007. (C) Lorentzian logarithmic symmetrical distribution centered at 1.9 ns. Full width at half-maximum was ~2.6 ns. The χ^2 value for this simulation was 1.008. (D) Third-degree polynomial function. The χ^2 value for this simulation was 1.008.

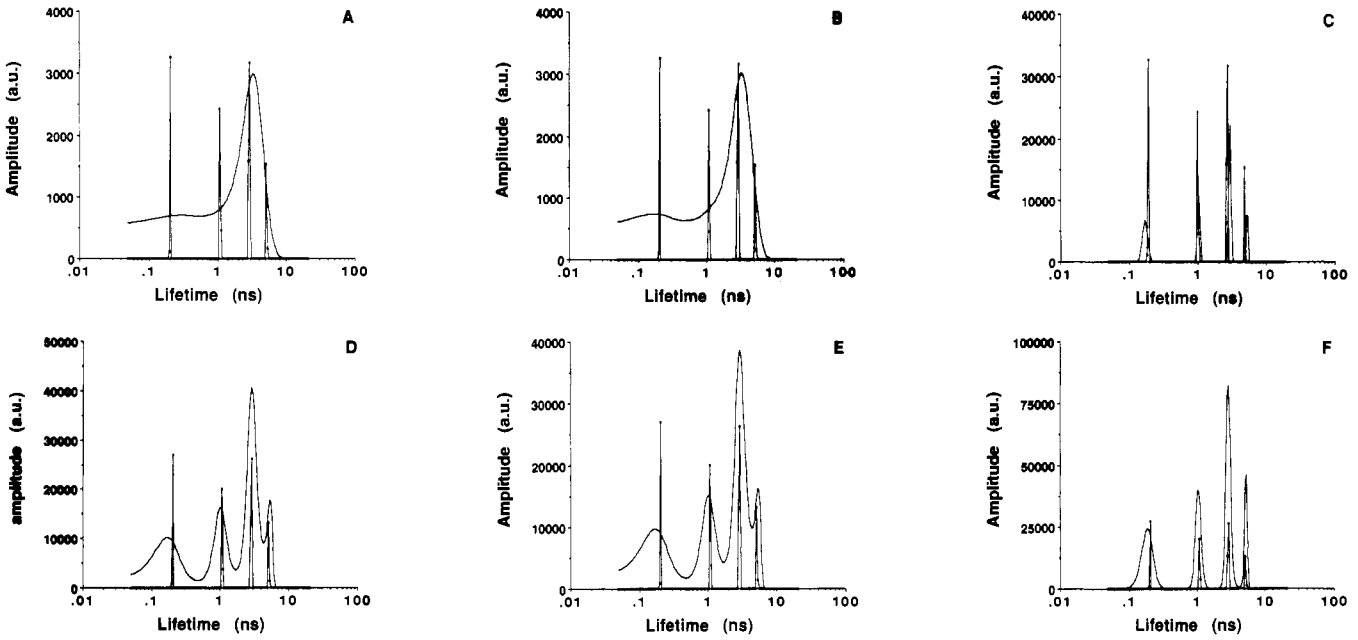

FIGURE 2: Amplitude profiles of the simulated discrete distributions of four exponentials recovered by MEM. (■) Original simulation. The parameters of the four exponential simulation were $\alpha_1 = 0.27$, $\tau_1 = 0.20$ ns; $\alpha_2 = 0.23$, $\tau_2 = 1.07$; $\alpha_3 = 0.37$, $\tau_3 = 2.86$; $\alpha_4 = 0.13$, $\tau_4 = 5.12$. Except for panel C, the amplitude axis of the original simulation was reduced by a factor 10. The χ^2 values for these simulations were 1.015 and 1.008 for the simulations with 60 000 and 500 000 counts in the peak channel, respectively. (A) 60 000 counts in the peak channel. (—) Amplitude profile obtained at the χ^2 value of the simulation. (B) 60 000 counts in the peak channel. (—) Amplitude profile obtained at the empirical criterion. The corresponding χ^2 value was 1.010. (C) 60 000 counts in the peak channel. (—) Amplitude profile obtained when the data are overfitted. The χ^2 value was 0.9839. (D) 500 000 counts in the peak channel. (—) Amplitude profile obtained at the χ^2 value of the simulation. (E) 500 000 counts in the peak channel. (—) Amplitude profile obtained at the empirical criterion. The corresponding χ^2 value was 1.011. (F) 500 000 counts in the peak channel. (—) Amplitude profile obtained when the data are overfitted. The χ^2 value was 0.9805.

to the mean over the 10th preceding iterations; such an amplitude profile was accepted as a conservative image of the "real" solution.

It is important to point out that, on the basis of this empirical stopping criterion, the only unrecovered simulated system is the four discrete exponential one when 60 000 counts in the peak channel are synthesized (Figure 2B) and that no significant difference can be observed when the profile obtained when MEM is stopped at the known χ^2 value (Figure 2A). The recovery of the different continuous lifetime distributions by using the empirical stopping criterion is quite acceptable, as shown in Figure 3. Major overfitting and consequently structuration of continuous profiles are avoided. However, by carrying on the analysis of the less cumulated simulated data (60 000 counts in the peak channel) beyond the profile obtained by using the stopping criterion or corresponding to the χ^2 value of the simulation, MEM can recover the four discrete simulated species (Figure 2C). The peak position and weighting of each species (the relative area over each peak) for the simulation involving 60 000 counts in the peak channel are very close to the respective ones from the analysis of the highly counted simulated curve (500 000 counts in the peak channel) at the expected χ^2 (Figure 2D), by using the stopping criterion (Figure 2E) or by overfitting the data (Figure 2F). This prompted us, at first, to cumulate experimental total fluorescence intensity curves at high level (typically 500 000 counts in the peak channel), which, in the absence of any information on the nature of the excited-state distribution (continuous or discontinuous) and with regard to the simulation conclusions, seems to represent the best current experimental approach for a minimal confident analysis by MEM.

Apocytochrome c Total Fluorescence Intensity Decays. The Trp-59 in apocytochrome *c* displayed a fluorescence emission maximum around 350 nm, indicating an accessible location with regard to the aqueous solvent on the average as reported in previous studies (Fisher et al., 1973; Rietveld et al., 1985). The total fluorescence intensity decay of this residue is clearly multiexponential. Nonlinear least-squares regression analysis of the decay requires at least three exponentials (Figure 4). A quadruple exponential model reduces the χ^2 value significantly (Table I). Analysis of the decay by MEM (Brochon & Livesey, 1988; Livesey et al., 1987; Livesey & Brochon, 1987), using the above-described stopping criterion, seems to credit the existence of four classes of lifetimes centered around 0.2, 1, 3, and 5 ns for the total fluorescence intensity decays culminating at 500 000 counts (Figure 5C). As in the simulations involving four discrete exponentials, not enough information is contained in the less cumulated curves (Figure 5A). Nevertheless, again as it was shown in the simulations, overfitting of the experimental decay curves leads to similar value of barycenter and area for each peak (Figure 5B,D). Moreover, the lifetimes as well as the fractional amplitude values obtained by MEM are in close agreement with those obtained by the nonlinear least-squares method.

Measurements at different excitation wavelengths in the red edge of the Trp absorption region do not evidence any significant change in the decay parameters (Table I). Emission wavelength dependence of the total intensity decay was monitored in three regions of the emission spectrum: 338, 358, and above 399 nm. In all cases, four classes of lifetimes are recovered by MEM. The decay values remain essentially unchanged within the experimental errors, but a redistribution of the fractional amplitudes between the two shortest and the two longest time components is observed (Table II). These last two components are favored at long wavelengths. This was observed at two widely different protein concentrations.

To get more insight into the relaxation mechanism of the Trp-59 excited-state properties, measurements of the total intensity decay were performed at different temperatures over

Table I: Total Fluorescence Intensity Decay Parameters of Trp-59 of Apocytochrome *c* as a Function of the Excitation Wavelength[a]

λ_{exc} (nm)	τ_1 (ns)	τ_2 (ns)	τ_3 (ns)	τ_4 (ns)	α_1	α_2	α_3	α_4	$\langle\tau\rangle$[e] (ns)	χ^2
292.5	0.38 ± 0.03[b]	2.06 ± 0.05	4.45 ± 0.04		0.31 ± 0.01	0.43 ± 0.01	0.26 ± 0.01			1.33
	0.18 ± 0.05[c]	1.18 ± 0.17	2.91 ± 0.29	4.95 ± 0.25	0.27 ± 0.02	0.26 ± 0.03	0.34 ± 0.02	0.13 ± 0.04	3.25	1.22
	0.18[d]	1.23	3.09	5.20	0.28	0.27	0.35	0.10		1.11
295	0.56 ± 0.03[b]	2.31 ± 0.06	4.65 ± 0.01		0.31 ± 0.03	0.45 ± 0.01	0.24 ± 0.01			1.36
	0.21 ± 0.07[c]	1.10 ± 0.14	2.92 ± 0.20	5.08 ± 0.20	0.20 ± 0.02	0.27 ± 0.02	0.39 ± 0.01	0.14 ± 0.03	3.30	1.26
	0.19[d]	1.04	2.85	4.96	0.19	0.26	0.41	0.14		1.16
300	0.43 ± 0.02[b]	2.25 ± 0.04	4.67 ± 0.04		0.34 ± 0.01	0.43 ± 0.01	0.23 ± 0.01			1.64
	0.21 ± 0.05[c]	1.05 ± 0.17	2.78 ± 0.18	5.02 ± 0.15	0.26 ± 0.02	0.22 ± 0.02	0.37 ± 0.02	0.15 ± 0.02	3.34	1.52
	0.21[d]	1.07	2.86	5.12	0.27	0.23	0.37	0.13		1.33

[a] Protein concentration: 139 μM. Temperature: 20 °C. Emission: 1 M $CuSO_4$ filter (2-cm optical path). Excitation bandwidth: 1 nm. The statistical errors were computed from the diagonal elements of the error matrix (Bevington, 1969). Footnotes *b–d* cited in column 2 apply to the values in columns 3–11 as well. [b] Nonlinear least-squares regression analysis with three exponentials. [c] Nonlinear least-squares regression analysis with four exponentials. [d] MEM analysis for which the τ_j (moment of order 1) over each peak are given (eq 7 under Materials and Methods). [e] The mean excited-state lifetime was calculated as $\langle\tau\rangle = \sum_i \alpha_i \tau_i^2 / \sum_i \alpha_i \tau_i$.

Table II: Total Fluorescence Intensity Decay Parameters of Trp-59 of Apocytochrome *c* as a Function of the Emission Wavelength[a]

apo *c* (μM)	λ_{em} (nm)	τ_1 (ns)	τ_2 (ns)	τ_3 (ns)	τ_4 (ns)	α_1	α_2	α_3	α_4	$\langle\tau\rangle$[e] (ns)	χ^2
1.8	338	0.32 ± 0.01[b]	2.03 ± 0.03	4.49 ± 0.01		0.49 ± 0.01	0.33 ± 0.03	0.18 ± 0.04			2.70
		0.16 ± 0.02[c]	0.99 ± 0.09	2.77 ± 0.13	5.01 ± 0.13	0.46 ± 0.03	0.21 ± 0.01	0.25 ± 0.01	0.08 ± 0.01	3.06	2.32
		0.15[d]	1.02	2.91	5.24	0.47	0.21	0.24	0.08		1.58
	358	0.36 ± 0.01[b]	2.25 ± 0.03	4.68 ± 0.03		0.47 ± 0.05	0.36 ± 0.03	0.17 ± 0.05			1.92
		0.22 ± 0.02[c]	1.12 ± 0.02	2.99 ± 0.13	5.38 ± 0.18	0.42 ± 0.01	0.20 ± 0.01	0.31 ± 0.01	0.07 ± 0.01	3.17	1.59
		0.20[d]	0.94	2.59	4.56	0.41	0.17	0.28	0.14		1.09
	399	0.40 ± 0.01[b]	2.52 ± 0.03	4.97 ± 0.04		0.35 ± 0.05	0.46 ± 0.05	0.19 ± 0.07			1.55
		0.18 ± 0.04[c]	1.03 ± 0.14	2.98 ± 0.11	5.46 ± 0.16	0.31 ± 0.02	0.18 ± 0.01	0.41 ± 0.01	0.11 ± 0.02	3.45	1.35
		0.17[d]	1.00	2.99	5.53	0.31	0.17	0.41	0.11		1.14
139	338	0.39 ± 0.01[b]	2.15 ± 0.03	4.62 ± 0.03		0.45 ± 0.05	0.37 ± 0.03	0.18 ± 0.05			1.45
		0.29 ± 0.02[c]	1.35 ± 0.12	3.09 ± 0.21	5.33 ± 0.25	0.40 ± 0.03	0.24 ± 0.01	0.28 ± 0.01	0.08 ± 0.02	3.12	1.25
		0.28[d]	1.37	3.18	5.45	0.41	0.24	0.28	0.07		1.06
	358	0.37 ± 0.01[b]	2.20 ± 0.03	4.63 ± 0.03		0.41 ± 0.06	0.39 ± 0.03	0.20 ± 0.05			1.70
		0.16 ± 0.03[c]	1.41 ± 0.05	3.39 ± 0.10	5.35 ± 0.16	0.44 ± 0.01	0.23 ± 0.02	0.29 ± 0.03	0.04 ± 0.02	3.22	1.41
		0.18[d]	1.43	3.41	5.36	0.44	0.23	0.29	0.04		1.21
	399	0.48 ± 0.02[b]	2.41 ± 0.04	4.70 ± 0.03		0.34 ± 0.01	0.41 ± 0.01	0.24 ± 0.01			1.83
		0.25 ± 0.04[c]	1.19 ± 0.13	3.18 ± 0.17	5.34 ± 0.03	0.27 ± 0.01	0.23 ± 0.01	0.39 ± 0.01	0.11 ± 0.03	3.42	1.63
		0.24[d]	1.14	3.12	5.04	0.26	0.23	0.39	0.12		1.39

[a] Excitation wavelength: 300 nm (bandwidth, 2 nm). Emission wavelengths were selected through a combination of filters including in each case a 1 M $CuSO_4$ cutoff filter (1-cm optical path). The second filters were, for 338 nm, a Schott interference filter UV-PIL (bandwidth, 5 nm; transmission coefficient, 0.28), for 358 nm, a M.T.O. interference filter Intervex I (bandwidth, 6 nm; transmission coefficient, 0.38), and for 399 nm, a Schott cutoff filter KV 399. Temperature: 20 °C. Footnotes *b–d* cited in column 3 apply to the values in columns 4–12 as well. [b] Analysis by nonlinear least-squares regression with three exponentials. [c] Analysis by nonlinear least-squares regression with four exponentials. [d] MEM analysis for which the τ_j (moment of order 1) over each peak is presented (eq 7 under Materials and Methods) except for τ_4 at 399 nm for which the peak maximum value is given. [e] $\langle\tau\rangle$ is defined in Table I.

Table III: Effect of Temperature on the Total Fluorescence Intensity Decay Parameters of Trp-59 of Apocytochrome *c*[a]

apo *c* (μM)	*T* (°C)	τ_1 (ns)	τ_2 (ns)	τ_3 (ns)	τ_4 (ns)	α_1	α_2	α_3	α_4	$\langle\tau\rangle$[d] (ns)
10.2	10	0.10 ± 0.02[b]	1.01 ± 0.07	3.21 ± 0.09	6.07 ± 0.10	0.43 ± 0.03	0.16 ± 0.01	0.29 ± 0.04	0.11 ± 0.01	4.03
		0.10[c]	0.96	3.16	5.77	0.41	0.18	0.30	0.11	
	25	0.14 ± 0.01[b]	1.20 ± 0.05	3.11 ± 0.07	6.43 ± 0.22	0.43 ± 0.02	0.22 ± 0.01	0.32 ± 0.01	0.03 ± 0.01	3.03
		0.13[c]	1.08	2.95	5.53	0.44	0.19	0.34	0.03	
	35	0.18 ± 0.03[b]	1.03 ± 0.06	2.59 ± 0.06	5.92 ± 0.19	0.33 ± 0.02	0.29 ± 0.01	0.35 ± 0.01	0.03 ± 0.04	2.52
		0.17[c]	1.07	2.69	7.30	0.34	0.30	0.35	0.01	
139	15	0.14 ± 0.03[b]	1.06 ± 0.10	2.94 ± 0.13	5.35 ± 0.10	0.31 ± 0.03	0.21 ± 0.01	0.33 ± 0.01	0.15 ± 0.02	3.61
		0.14[c]	1.07	2.98	5.38	0.32	0.21	0.33	0.14	
	20	0.15 ± 0.02[b]	1.25 ± 0.07	3.21 ± 0.14	5.52 ± 0.22	0.38 ± 0.02	0.24 ± 0.01	0.31 ± 0.01	0.07 ± 0.02	3.27
		0.15[c]	1.27	3.33	5.83	0.38	0.25	0.32	0.05	
	40	0.10 ± 0.01[b]	1.04 ± 0.03	2.53 ± 0.04	5.60 ± 0.21	0.40 ± 0.03	0.33 ± 0.01	0.26 ± 0.01	0.01 ± 0.02	2.05
		0.08[c]	1.04	2.47	5.69	0.42	0.31	0.26	0.01	

[a] Excitation wavelength: 295 nm (bandwidth, 2 nm). Emission: cutoff filter 1 M $CuSO_4$ (1-cm optical path). Footnotes *b* and *c* cited in column 3 apply to the values in columns 4–11 as well. [b] Nonlinear least-squares analysis with four exponentials. [c] MEM analysis for which the τ_j (moment of order 1) over each peak are given (eq 7 under Materials and Methods). [d] $\langle\tau\rangle$ is defined in Table I.

the full emission spectrum. The results are shown on Table III. At each protein concentration, the lifetime values remain essentially unchanged with the rise in temperature, except for the third component, which is depressed by about 15%. The main temperature effect is to almost cancel the contribution of the longest time component (α_4) at both protein concentrations tested (10.2 and 139 μM). Within the experimental error, this decrease parallels the rise in the amplitude of the second time component (α_2). The α_1 value is also modified but in the opposite way depending on the protein concentration (Table III).

Fluorescence Anisotropy Measurements. The Trp-59 fluorescence anisotropy decay cannot be satisfactorily fitted by a biexponential model as shown in Figure 6A. A third component is needed to minimize the χ^2 value and to randomize the deviation function as shown in Figure 6B. This

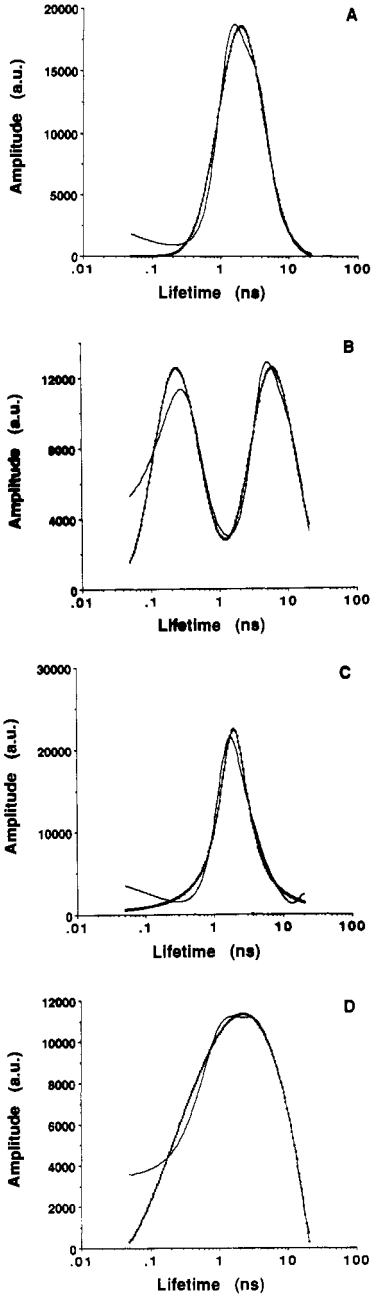

FIGURE 3: Amplitude profiles of the simulated continuous distributions of 150 exponentials recovered by MEM at the empirical criterion. 500 000 counts in the peak channel of all simulations. (■) Original simulation. (—) Profile recovered by MEM at the empirical criterion. (A) Gaussian logarithmic symmetrical distribution as in Figure 1A. The χ^2 value corresponding to the amplitude profile obtained was 1.008. (B) Double-Gaussian logarithmic symmetrical distribution as in Figure 1B. The χ^2 value corresponding to the amplitude profile obtained was 0.998. (C) Lorentzian logarithmic symmetrical distribution as in Figure 1C. The value corresponding to the amplitude profile obtained was 0.991. (D) Third-degree polynomial function. The χ^2 value corresponding to the amplitude profile obtained was 0.998.

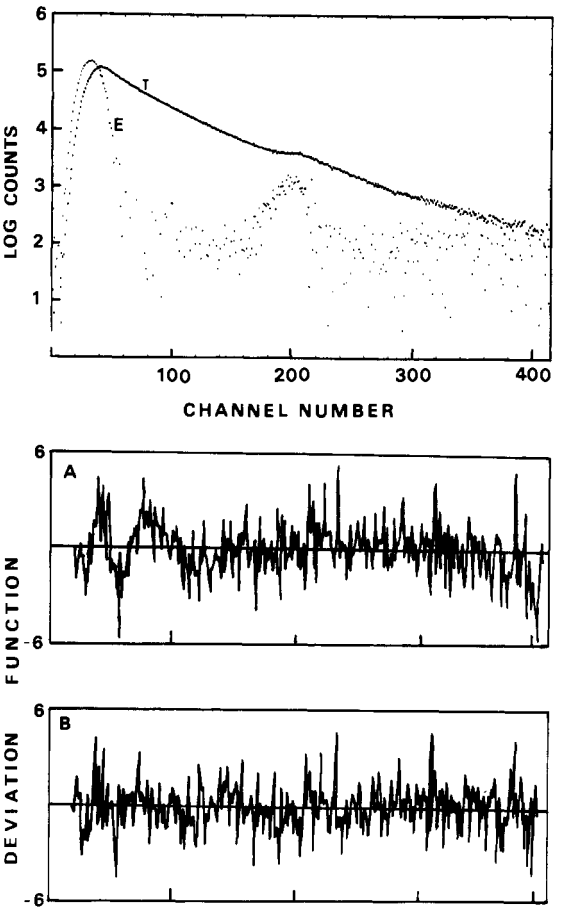

FIGURE 4: Total fluorescence intensity decay of Trp-59 of apocytochrome *c* (1.8 μM). Excitation wavelength: 298 nm (bandwidth, 2 nm). Emission: Schott interference filter UV-PIL (338 nm; bandwidth, 5 nm) and 1 M $CuSO_4$ cutoff filter (1-cm optical path). Time resolution: 0.080 ns/channel. Temperature: 20 °C. (Upper panel) (E) Instrument response function derived from *p*-terphenyl decay curve in cyclohexane; (T) experimental decay. (Lower panels) Deviation functions for (A) triple exponential model ($\alpha_1 = 0.47 \pm 0.01$, $\tau_1 = 0.36 \pm 0.01$ ns; $\alpha_2 = 0.36 \pm 0.01$, $\tau_2 = 2.25 \pm 0.03$ ns; $\alpha_3 = 0.17 \pm 0.01$, $\tau_3 = 4.69 \pm 0.03$ ns; $\chi^2 = 2.13$) and (B) quadruple exponential model ($\alpha_1 = 0.43 \pm 0.01$, $\tau_1 = 0.23 \pm 0.02$ ns; $\alpha_2 = 0.20 \pm 0.01$, $\tau_2 = 1.16 \pm 0.11$ ns; $\alpha_3 = 0.30 \pm 0.01$, $\tau_3 = 3.02 \pm 0.13$ ns; $\alpha_4 = 0.07 \pm 0.01$, $\tau_4 = 5.43 \pm 0.19$ ns; $\chi^2 = 1.82$).

is found for each protein concentration tested (2.1, 8.5, and 139 μM) (Table IV). In order to investigate whether the existence of energy transfer would be in part responsible for the shortest correlation time, the anisotropy decays were measured at different excitation wavelengths in the red edge of the Trp absorption region for two widely different protein concentrations. Whatever the concentration, there is no significant effect of the excitation wavelength on the correlation time values and on the relative contribution of the shortest correlation time (Table IV). Only for 292.5-nm excitation wavelength and high protein concentration can a significant increase of the short correlation time contribution be observed. Whatever the excitation wavelength and the protein concentration, the $r_{0,\text{eff}}$ values are always lower than the value measured in vitrified glycerol (Figure 7). As a function of the protein concentration, the shortest correlation time remains essentially unchanged, whereas the intermediate one is enhanced (Table IV). The value of the third correlation time increases as a function of the protein concentration from 5 to around 10 ns. Steady-state anisotropy values measured as a function of the protein concentration increase from 0.037 at 3.5 μM to 0.096 at 40 μM; above this concentration a plateau is observed (Figure 8). In this protein concentration range, the mean excited-state lifetime remains constant. Upon addition of urea (3.7 or 8 M) to a 139 μM apocytochrome *c* solution, the long correlation time values, corrected for the viscosity effect of urea, decrease to values similar to those found in buffer at low protein concentration (Table IV).

Discussion

There is now a large set of experimental data showing that proteins containing a single tryptophan residue exhibit nonmonoexponential total fluorescence emission decays (Ludescher

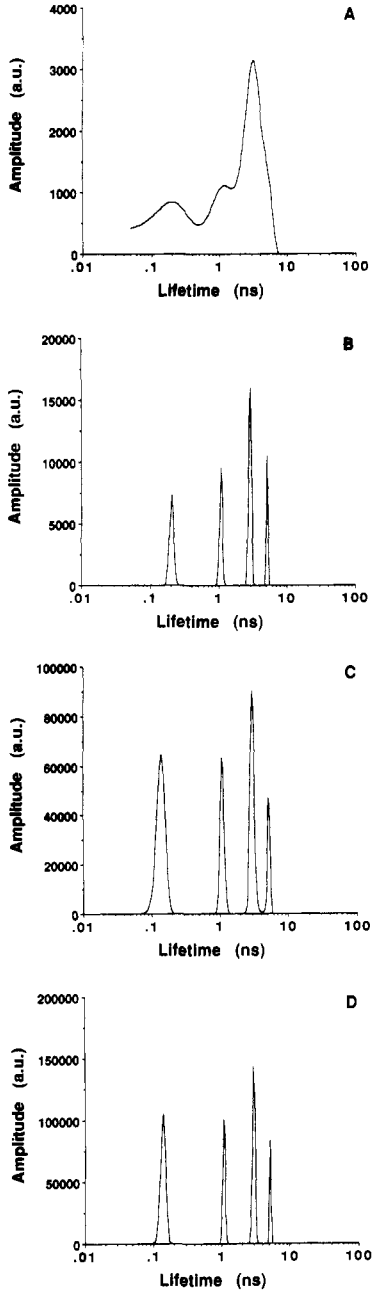

FIGURE 5: Amplitude profiles of apocytochrome *c* total fluorescence intensity decay recovered by MEM. Apocytochrome *c* concentration: 139 μM. Excitation wavelength: 300 nm (bandwidth, 2 nm). Emission: $CuSO_4$ cutoff filter (2-cm optical path). Temperature: 20 °C. (A) 60 000 counts in the peak channel. Amplitude profile obtained at the empirical criterion. The corresponding χ^2 value was 1.367. (B) 60 000 counts in the peak channel. Amplitude profile obtained when the data are overfitted. The corresponding χ^2 value was 1.353. (C) 500 000 counts in the peak channel. Amplitude profile obtained at the empirical criterion. The corresponding χ^2 value was 2.022. (D) 500 000 counts in the peak channel. Amplitude profile obtained when the data are overfitted. The corresponding χ^2 value was 2.015.

et al., 1985; Lakowicz et al., 1984; Beechem & Brand, 1985). This is attributed to the complexity of the indole and derivative photophysics, the radiative and nonradiative deactivation pathways being modulated by the interactions of the indole ring with the amino acid side-chain residues of its environment (Creed, 1984). Moreover, the existence of ground-state conformers of the tryptophan residue in proteins and of solvent or protein matrix reorientation around the chromophore excited state have to be considered.

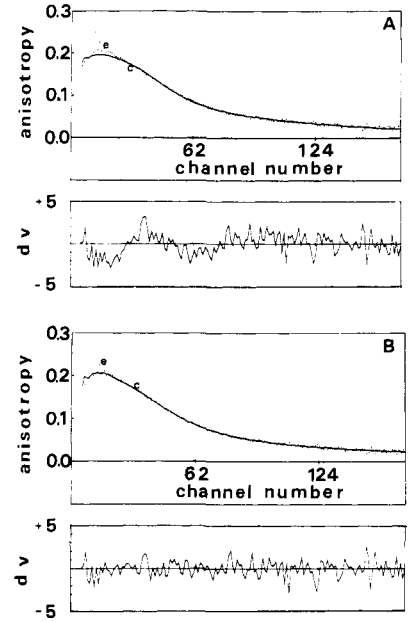

FIGURE 6: Time-resolved fluorescence anisotropy decay of Trp-59 of apocytochrome *c* (139 μM). Experimental conditions are as in Figure 5. $\sim 10^5$ counts were cumulated in the peak channel of the difference $D(t)$. Time resolution: 0.080 ns/channel. (A) Biexponential model: $\beta_1 = 0.126$, $\theta_1 = 0.68$ ns; $\beta_2 = 0.098$, $\theta_2 = 6.72$ ns; $r_{0,eff} = 0.224$; $\chi^2 = 1.33$. (B) Triple exponential model: $\beta_1 = 0.102$, $\theta_1 = 0.12$ ns; $\beta_2 = 0.098$, $\theta_2 = 1.74$ ns; $\beta_3 = 0.064$, $\theta_3 = 10.06$ ns; $r_{0,eff} = 0.264$; $\chi^2 = 0.99$. (e, dotted line) Experimental points; (c, full curve) reconvolved curve; (DV) deviation function.

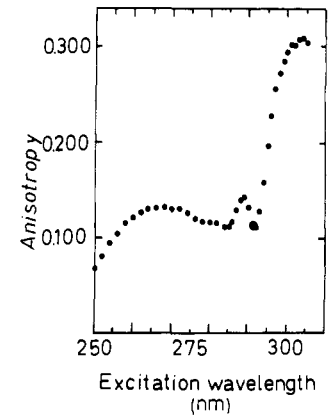

FIGURE 7: Intrinsic fluorescence anisotropy spectrum of Trp-59 of apocytochrome *c* in vitrified glycerol (−38 °C). A concentration of 10 μM protein in 91% glycerol (v/v) was used. Other conditions are described under Materials and Methods.

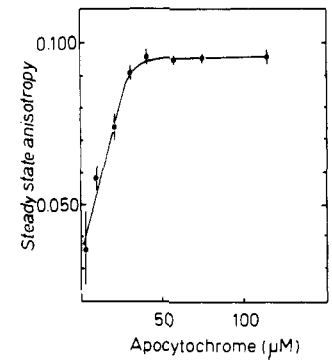

FIGURE 8: Steady-state fluorescence anisotropy as a function of apocytochrome *c* concentration. Buffer: 0.1 M acetate, pH 5. Temperature: 20 °C. Excitation wavelength: 300 nm (bandwidth, 1–4 nm). Emission: 1 M $CuSO_4$ cutoff filter (2-cm optical path).

Table IV: Time-Resolved Fluorescence Anisotropy Decay Parameters of Trp-59 in Apocytochrome *c* as a Function of Protein Concentration[a]

apo *c* (μM)	β_1	β_2	β_3	θ_1 (ns)	θ_2 (ns)	θ_3 (ns)	$r_{0,eff}$
1.8	0.080 ± 0.007[b]	0.078 ± 0.015	0.080 ± 0.020	0.14 ± 0.01	1.09 ± 0.17	5.33 ± 0.31	0.238 ± 0.040
8.5	0.088 ± 0.011[b]	0.077 ± 0.008	0.083 ± 0.003	0.18 ± 0.02	1.37 ± 0.04	6.25 ± 0.25	0.248 ± 0.011
	0.083 ± 0.018[c]	0.060 ± 0.008	0.059 ± 0.013	0.17 ± 0.07	1.33 ± 0.18	5.67 ± 0.34	0.200 ± 0.004
139	0.107 ± 0.017[b]	0.106 ± 0.008	0.065 ± 0.004	0.17 ■ 0.03	1.72 ± 0.11	9.41 ± 0.39	0.278 ± 0.023
	0.078 ± 0.017[c]	0.067 ± 0.008	0.043 ± 0.007	0.24 ± 0.07	1.89 ± 0.13	8.77 ± 1.35	0.188 ± 0.005
	0.074 ± 0.004[d]	0.047 ± 0.006	0.033 ± 0.010	0.25 ± 0.06	1.87 ± 0.53	7.86 ± 1.70	0.154 ± 0.024
139[e]	0.127 ± 0.012[b]	0.110 ± 0.003	0.043 ± 0.001	0.18 ± 0.03	1.52 ± 0.04	6.99 ± 0.23	0.280 ± 0.009
				0.15[g]	1.28[g]	5.87[g]	
139[f]	0.139 ± 0.013[b]	0.109 ± 0.005	0.041 ± 0.008	0.15 ± 0.04	1.73 ± 0.18	7.19 ± 0.97	0.289 ± 0.026
				0.09[g]	1.04[g]	4.33[g]	

[a] Emission: cutoff filter 1 M $CuSO_4$ (2-cm optical path). Triple exponential model: $r(t) = \beta_1 \exp(-t/\theta_1) + \beta_2 \exp(-t/\theta_2) + \beta_3 \exp(-t/\theta_3)$. The results are expressed as mean values ± SD over two to five determinations. Temperature: 20 °C. Footnotes *b–d* cited in column 2 apply to the values in columns 3–8 as well. [b] Excitation wavelength: 300 nm (2-nm bandwidth). [c] Excitation wavelength: 295 nm (2-nm bandwidth). [d] Excitation wavelength: 292.5 nm (2-nm bandwidth). [e] In presence of 3.7 M urea. [f] In presence of 8 M urea. [g] Values corrected for the viscosity effect of urea (viscosity = 1.19 and 1.66 cP for 3.7 and 8 M, respectively).

In the case of apocytochrome *c*, the analysis of the highly cumulated total intensity decay curves by MEM is in favor of the existence of at least four separate classes of excited-state lifetimes, taking into account the present experimental conditions. Instead of dealing with values representing the mean and width of an underlying continuous distribution of lifetimes (Ludescher et al., 1985; James & Ware, 1985, 1986; Alcala et al., 1987a–c), it is likely that the total intensity decay data of apocytochrome *c* can be interpreted by a set of four classes of excited-state lifetimes, since from simulation conclusions MEM can satisfactorily recover broad distributions.

The decay parameters of Trp-59 cannot be ascribed to ground-state species displaying slightly different absorption spectra since they do not change with the excitation wavelength. The measurements performed at excitation wavelength in the red edge of the absorption spectrum (300 nm) allow one to exclude the existence of Trp–Trp energy transfer in the high concentration range of the protein (Weber & Shinitzky, 1970). The anisotropy decay data measured in the same experimental conditions further support this point, as will be discussed later on. The possibility of solvent or peptide group relaxation (DeToma et al., 1976; Lakowicz & Cherek, 1980) effective during the Trp excited-state lifetime is questionable since the center value of each class of lifetimes remains invariant within the experimental errors as a function of the emission wavelength. Instead, we observed a redistribution of amplitudes between the classes corresponding to the two shortest and the two longest time components as a function of the emission wavelength. A tempting explanation would be the existence of defined ground states with slightly different emission spectra. In agreement with this interpretation, temperature displays a selective effect: it swung the fractional contribution of the longest time component to the benefit of either the 1-ns component alone or the two shortest components, depending on the associated state of the protein, without affecting to a large extent the lifetime values themselves. This suggests that Trp-59 interconverting environments are occurring. They could correspond to conformational substates of apocytochrome *c* in thermal equilibrium slow to exchange within the fluorescence time scale. The rates of exchange must be roughly 5 times the value of the longest time component as suggested by Engh et al. (1986).

The examination of the primary sequence of horse heart apocytochrome *c* allows one to propose a tempting model to partially explain the Trp-59 emission heterogeneity. The structural predictions performed according to the method of Chou and Fasman (1978) as reported recently (Rietveld et al., 1985), in agreement with earlier statements (Prothero, 1966; Schiffers & Edmundson, 1967), suggest that the Trp-59 residue is located in the N-terminal part of an α-helical segment of 12 amino acid residues extending from Thr-58 to Glu-69. In the cytochrome *c* crystal, this portion of the chain is in fact almost helical (Dickerson et al., 1971). According to the predictions, this segment is intercalated between two β-turns. Therefore, the Trp-59 residue is situated in a potentially structure-forming region. One can suggest that there might be interactions with Glu-61 and Glu-62 side chains in a transiently forming helical structure. This could give rise to the short time components that are blue-shifted as compared to the longest lifetime emitting species. According to Szabo and Rayner (1980), the interactions of the indole nucleus with carboxyl groups could destabilize the excited state and lead to fluorescence emission at higher energies. Alternatively, the short lifetimes might correspond to transient environments less accessible to the solvent. In each of these substates, the indole ring can occupy different "rotameric" or "conformeric" positions with respect to the C_α–C_β and C_β–C_γ bonds (Szabo & Rayner, 1980; Chang et al., 1983; Petrich et al., 1983; Ross et al., 1981; Engh et al., 1986), following earlier statements (Gauduchon & Wahl, 1978; Donzel et al., 1974).

The high signal to noise ratio of the experimental anisotropy decay data ($\sim 10^5$ counts in the difference curve) allowed an analysis by three correlation times for χ^2 minimization. This was observed for two widely different protein concentrations. According to Ichiye and Karplus (1983), an expression of the time-dependent anisotropy can be

$$r(t) = r_0[(1 - P_\infty^1) \exp(-t/\theta_1) + P_\infty^1] \times [(1 - P_\infty^2) \exp(-t/\theta_2) + P_\infty^2] \exp(-t/\theta_m)$$

where θ_1 and θ_2 are two correlation times describing the internal motions and θ_m is the correlation time of the whole protein. This expression corresponds to a correlation function for the internal motion that separates into two time scales. If $\theta_1 \ll \theta_2 \ll \theta_m$, this expression can be reduced to a sum of three exponentials (Ichiye & Karplus, 1983)

$$r(t) = \beta_1 \exp(-t/\theta_1) + \beta_2 \exp(-t/\theta_2) + \beta_3 \exp(-t/\theta_m)$$

with coefficients $\beta_1 = (1 - P_\infty^1)r_0$, $\beta_2 = P_\infty^1 (1 - P_\infty^2)r_0$, and $\beta_3 = P_\infty^1 P_\infty^2 r_0$.

From the β_1 value it is possible to calculate an average angular displacement for the Trp-59 transition moment of around 55° (Kinosita et al., 1977), almost invariant with the protein concentration. This is larger than was previously found for flexible peptides like synthetic adrenocorticotropin (1–24) or glucagon (Tran et al., 1982; Gallay et al., 1987; Chen et al., 1987) but is of the same order of magnitude as for the monomeric mellitin (Tran & Beddard, 1985; Lakowicz et al., 1987). This indeed points to the fact that the angular dis-

placement undergone by the Trp-59 in apocytochrome *c* is very large and fast and emphasizes the high flexibility of this protein. However, by contrast to another highly flexible protein, namely, the myelin basic protein (Munro et al., 1979), the fast internal rotation does not account for the total depolarization of the exciting light in apocytochrome *c* since the long correlation time corresponding to the rotational motion of the whole protein can be detected in our anisotropy decay measurements. Therefore, this suggests the existence of a remaining local structure in the vicinity of the Trp-59 residue, where specific interactions are occurring as indicated by the lifetime measurements. The second internal correlation time would arise from local flexibilities of the peptide chain involving the Trp-59 residue. The existence of such motions has also been suggested in the case of mellitin (Lakowicz et al., 1987) and also for the myelin basic protein (Munro et al., 1979).

The overall motion of the protein, represented by θ_m, is sensitive to protein concentration. At low protein concentrations, a correlation time of 5 ns was observed, which can be considered reasonable in view of the molecular weight of the protein (11 900) assumed as a rotating sphere with an hydration ratio of about 30–40% (w/w). The correlation time value is almost doubled at high protein concentration. A likely interpretation would be the formation of a dimer as a function of protein concentration. The existence of a minor population of higher oligomers has been evidenced in previous work (Stellwagen et al., 1972; Fisher et al., 1973; Dumont & Richards, 1984; Rietveld et al., 1985), but these oligomers were not detected in the present work, which was performed at relatively low protein concentrations. The association process is also detectable by steady-state anisotropy measurements.

In the associated form of the protein, the Trp-59 environment seems to be not deeply modified in terms of lifetimes and fast internal rotation. We have to note that if the short correlation time were the result of Trp–Trp energy transfer in this state of the protein, a variation of its relative contribution would have been observed as a function of the excitation wavelength in the specific absorption spectrum region of the chromophore (Weber & Shinitzky, 1970), which was not the case in our data. A significant increase of the short correlation time contribution was noticeable only at 292.5-nm excitation wavelength, which could be attributed to Tyr–Trp energy transfer or to monitoring of a different rotation of the indole ring since the ^1L_a and the ^1L_b transitions are perpendicular to each other (Yamamoto & Tanaka, 1972). The local motion attributed to peptide chain deformation is slower and its contribution to the anisotropy increases in the associated form. This form is disrupted by addition of urea from 3.7 to 8 M. This indicates that only weak interactions are likely to stabilize this state of the protein. Examination of the primary sequence and of the hydrophobic plot of apocytochrome *c* (Rietveld et al., 1985) suggests that the C-terminal end may be involved in the self-association process since it is the less electrostatically charged region of the protein.

In conclusion, we propose that, by taking advantage of the maximum entropy method, the Trp-59 emission of horse heart apocytochrome *c* can be characterized by distributions of at least four excited-state lifetime classes. By contrast to other methods used for lifetime distribution recovery (James & Ware, 1986; James et al., 1987), MEM can handle much larger exponential series (typically 200 instead of 20). Moreover, there is no need with MEM to remove preexponential terms of values close to zero during the iterative optimization process.

The accuracy of MEM analysis suggests the existence of discrete conformational substrates of apocytochrome *c* in thermal equilibrium in aqueous solutions. We can speculate that some of these conformational substates may be selected at the membrane interface to facilitate heme fixation. Fluorescence anisotropy decay measurements emphasize a fast internal motion of large amplitude for the Trp residue and a slower peptide chain flexibility of the segment including this residue. They also evidence an association process starting at low protein concentration, leading, in the conditions of this work, mainly to a dimer. However, the anisotropy decay data were analyzed by considering the populations of the fluorophores as being homogeneous in terms of rotational motions. Such an assumption can be tested by extending the one-dimensional analysis (eq 3) to the three-dimensional one (eq 1 or 2, or 1 and 2 sequentially) (Brochon & Livesey, 1987).

ACKNOWLEDGMENTS

We are greatly indebted to Dr. A. K. Livesey for continuous helpful advice and discussions about the maximum entropy method and for critical reading of the manuscript. We gratefully acknowledge B. de Kruijff for helpful criticism and continuous interest in this work. We thank the technical staff of LURE for running the synchrotron machine during the beam-time sessions, and we appreciate the technical assistance of A. M. Faugère. Finally, we thank the referees for constructive suggestions about the simulations.

Registry No. Apo *c*, 9007-43-6; Trp, 73-22-3.

REFERENCES

Alcala, J. R., Gratton, E., & Prendergast, F. G. (1987a) *Biophys. J. 51*, 587–596.

Alcala, J. R., Gratton, E., & Prendergast, F. G. (1987b) *Biophys. J. 51*, 597–604.

Alcala, J. R., Gratton, E., & Prendergast, F. G. (1987c) *Biophys. J. 51*, 925–936.

Beechem, J. M., & Brand, L. (1985) *Annu. Rev. Biochem. 54*, 43–71.

Berkhout, T. A., Rietveld, A., & De Kruijff, B. (1987) *Biochim. Biophys. Acta 897*, 1–4.

Berlman, I. B. (1971) in *Handbook of Fluorescence Spectra of Aromatic Molecules*, p 220, Academic, New York.

Bevington, P. R. (1969) in *Data Reduction and Error Analysis for the Physical Sciences*, McGraw-Hill, New York.

Blundell, T., & Wood, S. (1982) *Annu. Rev. Biochem. 51*, 123–154.

Bornet, H., & Edelhoch, H. (1971) *J. Biol. Chem. 246*, 1785–1792.

Braun, W., Wider, G., Lee, K. H., & Wüthrich, K. (1983) *J. Mol. Biol. 169*, 921–948.

Brochon, J. C. (1980) in *Protein Dynamics and Energy Transduction* (Ishiwata, S., Ed.) Proceedings of the 6th Taniguchi International Symposium, Biophysic Division, pp 163–169, the Taniguchi Foundation, Tokyo.

Brochon, J. C., & Livesey, A. K. (1987) in *Proceedings of the 2nd Congress of the European Society for Photobiology*, Padova, Italy (Douglas, R. H., Moan, J., & Dall'Acqua, F., Eds.) (in press).

Brochon, J. C., & Livesey, A. K. (1988) in *Fluorescent Biomolecules* (Jameson, D., & Gratton, E., Eds.) (in press).

Chang, M. C., Petrich, J. W., McDonald, D. B., & Fleming, G. R. (1983) *J. Am. Chem. Soc. 105*, 3819–3824.

Chen, L. X.-Q., Petrich, J. W., & Fleming, G. R. (1987) *Chem. Phys. Lett. 139*, 55–61.

Chou, P. Y., & Fasman, G. D. (1978) *Adv. Enzymol. Relat. Areas Mol. Biol. 47*, 45–148.

Cohen, J. S., Fisher, W. R., & Shechter, A. N. (1974) *J. Biol. Chem. 249*, 1113–1118.
Creed, D. (1984) *Photochem. Photobiol. 39*, 537–562.
DeToma, T. P., Easter, J. H., & Brand, L. (1976) *J. Am. Chem. Soc. 98*, 5001–5007.
Dickerson, R. E., Takano, T., Eisenberg, D., Kallai, O. B., Samson, L., Cooper, A., & Margoliash, E. (1971) *J. Biol. Chem. 246*, 1511–1535.
Donzel, B., Gauduchon, P., & Wahl, Ph. (1974) *J. Am. Chem. Soc. 96*, 801–808.
Dumont, M. E., & Richards, F. M. (1984) *J. Biol. Chem. 259*, 4147–4156.
Engh, R. A., Chen, L. X.-Q., & Fleming, G. R. (1986) *Chem. Phys. Lett. 126*, 365–372.
Fisher, W. R., Taniushi, H., & Anfinsen, C. B. (1973) *J. Biol. Chem. 248*, 3188–3195.
Gallay, J., Vincent, M., Nicot, C., & Waks, M. (1987) *Biochemistry 26*, 5738–5747.
Gauduchon, P., & Wahl, Ph. (1978) *Biophys. Chem. 8*, 87–104.
Gremlich, H. U., Fringeli, P., & Schwyzer, R. (1983) *Biochemistry 22*, 4257–4264.
Grinvald, A., & Steinberg, I. Z. (1974) *Anal. Biochem. 59*, 583–598.
Hennig, B., Koehler, H., & Neupert, W. (1983) in *Mitochondria* (Schweyen, R. J., Wolff, K., & Kaudewitz, F., Eds.) pp 551–561, de Gruyter, Berlin.
Ichiye, T., & Karplus, M. (1983) *Biochemistry 22*, 2884–2893.
James, D. R., & Ware, W. R. (1985) *Chem. Phys. Lett. 120*, 450–454.
James, D. R., & Ware, W. R. (1986) *Chem. Phys. Lett. 126*, 7–11.
James, D. R., Turnbull, J. R., Wagner, B. D., Ware, W. R., & Petersen, N. O. (1987) *Biochemistry 26*, 6272–6277.
Jameson, D. M., & Alpert, B. (1979) in *Synchrotron Radiation Applied to Biophysical and Biochemical Research* (Castellman, A., & Quercia, I. F., Eds.) pp 183–201, Plenum, New York.
Jaynes, E. T. (1983) *Papers on Probability Statistics and Statistical Physics* (Rosenkrantz, R. D., Ed.) Reidel, Dordrecht, The Netherlands.
Kinosita, K., Kawato, S., & Ikegami, A. (1977) *Biophys. J. 20*, 289–305.
Lakowicz, J. R., & Cherek, H. (1980) *J. Biol. Chem. 225*, 831–834.
Lakowicz, J. R., Gratton, E., Laczko, G., Cherek, H., & Limkeman, M. (1984) *Biophys. J. 46*, 463–467.
Lakowicz, J. R., Cherek, H., Gryczynski, I., Joshi, N., & Johnson, M. L. (1987) *Biophys. J. 51*, 755–768.
Livesey, A. K., & Skilling, J. (1985) *Acta Crystallogr., Sect. A: Found. Crystallogr. A41*, 113–122.
Livesey, A. K., & Brochon, J. C. (1987) *Biophys. J. 52*, 693–706.
Livesey, A. K., Delahaye, M., Licinio, P., & Brochon, J. C. (1987) *Faraday Discuss. Chem. Soc.* (in press).
Ludescher, R. P., Volwerk, J. J., De Haas, G. H., & Hudson, B. S. (1985) *Biochemistry 24*, 7240–7249.
Munro, I., Pecht, I., & Stryer, L. (1979) *Proc. Natl. Acad. Sci. U.S.A. 76*, 56–60.
Petrich, J. W., Chang, M. C., McDonald, D. B., & Fleming, G. R. (1983) *J. Am. Chem. Soc. 105*, 3824–3832.
Prothero, J. W. (1966) *Biophys. J. 6*, 367–370.
Rietveld, A., Sijens, P., Verkleij, A. J., & De Kruijff, B. (1983) *EMBO J. 2*, 907–913.
Rietveld, A., Ponjee, G. A. E., Schiffers, Jordi, W., Van de Coolwick, P. J. F. M., Demel, R. A., Marsh, D., & De Kruijff, B. (1985) *Biochim. Biophys. Acta 818*, 398–409.
Ross, J. B. A., Rousslang, K. W., & Brand, L. (1981) *Biochemistry 20*, 4361–4369.
Schiffers, M., & Edmundson, A. B. (1967) *Biophys. J. 7*, 121–126.
Schiller, P. W. (1985) in *The Peptides* (Hruby, V. J., Ed.) pp 115–164, Academic, New York.
Schneider, A. B., & Edelhoch, H. (1972) *J. Biol. Chem. 247*, 4986–4991.
Stellwagen, E., Rysavy, R., & Babul, G. (1972) *J. Biol. Chem. 247*, 8074–8077.
Szabo, A. G., & Rayner, D. M. (1980) *J. Am. Chem. Soc. 102*, 554–563.
Tran, C. D., & Beddard, G. S. (1985) *Eur. J. Biophys. 13*, 59–64.
Tran, C. D., Beddard, G. S., & Osborne, A. D. (1982) *Biochim. Biophys. Acta 709*, 256–264.
Vincent, M., De Foresta, B., Gallay, J., & Alfsen, A. (1982) *Biochemistry 21*, 708–716.
Wahl, Ph. (1975) in *New Techniques in Biophysics and Cell Biology* (Pain, H., & Smith, H. B., Eds.) Vol. 2, pp 233–285, Wiley, London.
Wahl, Ph. (1979) *Biophys. Chem. 10*, 91–104.
Wand, A. J., & Englander, S. W. (1985) *Biochemistry 24*, 5290–5294.
Weber, G., & Teale, F. J. W. (1959) *Discuss. Faraday Soc. 27*, 134.
Weber, G., & Shinitzky, M. (1970) *Proc. Natl. Acad. Sci. U.S.A. 65*, 823–830.
Yamamoto, Y., & Tanaka, J. (1972) *Bull. Chem. Soc. Jpn. 65*, 1362–1366.
Yguerabide, J. (1972) *Methods Enzymol. 26*, 498–578.